EUROPEAN ORGANIZATION FOR NUCLEAR RESEARCH

A STUDY OF ALL THE $\pi\pi$ PHASE SHIFT SOLUTIONS IN THE MASS REGION 1.0 TO 1.8 GeV FROM $\pi^- p \to \pi^-\pi^+ n$ AT 17.2 GeV

B. Hyams, C. Jones and P. Weilhammer
CERN, Geneva, Switzerland

and

W. Blum, H. Dietl, G. Grayer, W. Koch, E. Lorenz, G. Lütjens, W. Männer, J. Meissburger, W. Ochs*) and U. Stierlin

Max-Planck-Institut für Physik und Astrophysik
Munich, Germany

ABSTRACT

The $\pi\pi$ phase shifts from 1 to 1.8 GeV are presented. The method used was an essentially energy-independent parametrization of the amplitudes fitted simultaneously to the $M_{\pi\pi}$ and t-dependence of the moments of the dipion angular distribution from the reaction $\pi^- p \to \pi^-\pi^+ n$ at 17.2 GeV.

The various ambiguous solutions are discussed.

Geneva - 30 April 1975
(Submitted to Nuclear Physics)

*) Now at the California Institute of Technology, Pasadena, California 91109.

1. INTRODUCTION

During the last years considerable effort has been invested in the study of $\pi\pi$ phase shifts.

After the determination of the dominating resonances ρ, f, g, the interest shifted to the study of the lower-lying partial waves. One remaining question is the existence of daughter trajectories. This problem still remains unsolved. While it is established that the S-wave goes through 90° under the ρ and f mesons[1], the change of phase is so slow that one is reluctant to describe this behaviour by poles in the T-matrix.

The determination of the P-wave at high $\pi\pi$ mass is problematic owing to the occurrence of ambiguities.

We study these problems with over 300,000 events from the reaction

$$\pi^- p \to \pi^- \pi^+ n \text{ at } 17.2 \text{ GeV} \tag{1}$$

obtained by our group[2].

Previous papers (see Ref. 2) have dealt with the phase shifts below 1 GeV. In our first study above this energy[3] we started from an energy-dependent amplitude analysis in the momentum transfer interval $|t_{min}| < |t| < 0.15$ GeV^2. If in addition to the leading resonances we included an S-wave resonance in the f-meson region and a P-wave resonance (ρ') in the g-meson region, reasonable agreement with the data was obtained. The parameters found in this fit were then used as starting values for a subsequent energy-independent fit. A classification of this solution was given in terms of the amplitude zeros, but no attempt had yet been made to fully explore the range of all possible solutions. In the present paper we discuss all occurring ambiguities. A different fitting procedure was applied which combines energy-dependent and energy-independent methods. We parametrize the leading resonances with a Breit-Wigner shape in order to determine the over-all phase. The lower-lying waves are described in an energy-independent way. We fit the mass- and t-dependence at the same time, using the complete error correlation matrix obtaining in that way more stringent constraints than those of Ref. 3. A first account of the present work has been presented previously[4]. Some results of a similar analysis by Estabrooks and Martin[5] became available recently. Instead of the partial wave amplitudes, these authors parametrize the amplitude zeros, as a consequence losing the constraints provided by unitarity and analyticity.

2. METHOD OF ANALYSIS

Since $\pi\pi$ scattering cannot be measured directly, it is important to discuss the methods employed.

The possibility to determine $\pi\pi$ scattering from existing experiments is given by the Chew-Low equation[6]:

$$\lim_{t\to M_\pi^2} \frac{\partial^2\sigma}{\partial M_{\pi\pi}\partial t} = \frac{M_{\pi\pi}^2 \cdot q}{4\pi M_p^2 p_{lab}^2} \frac{g^2}{4\pi} \frac{-t}{(M_\pi^2 - t)^2} \sigma_{\pi\pi} , \quad (2)$$

where

M_p, M_π, and $M_{\pi\pi}$ are the masses of the proton, pion, and outgoing dipion system, respectively;

p_{lab} is the beam momentum in the lab system;

$g^2/4\pi = 2 \times 14.6$ is the nucleon-pion-nucleon coupling constant;

$q = \sqrt{1/4\, M_{\pi\pi}^2 - M_\pi^2}$ is the momentum of the pions in the dipion centre of mass;

t is the momentum transfer to the nucleon; and

$\sigma_{\pi\pi}$ is the desired $\pi\pi$ cross-section.

In principle, this formula gives a model-independent way of determining $\pi\pi$ scattering. In practice, however, one relies on the fact that pion exchange is dominating in the physical region[2,7].

In order to extract as much information as possible from the experiment, we perform an amplitude analysis which relies on further assumptions.

i) Factorization

All amplitudes factorize into a part given by $\pi\pi$ scattering, not depending on t, but varying rapidly with $M_{\pi\pi}$ as determined by the $\pi\pi$ phase shifts, and a factor describing the production process which depends strongly on t, but whose $M_{\pi\pi}$ dependence is given by phase space only ($M_{\pi\pi}^2/q$).

In agreement with the data[2] this assumption is also applied to the $m = 1$ t-channel amplitudes, which should vanish for pure one-pion exchange.

ii) s-channel nucleon spin-flip dominance

In the absence of polarization measurements we cannot measure all amplitudes. As suggested by the authors of the "Poor Man's Absorption Model"[8], all analyses make the above assumption.

Experimental tests of this assumption can be made by studying the t-dependence at very low $t \approx t_{min}$. One can also evaluate the rank of the density matrix[9]. Rank 2 requires all unnatural exchange amplitudes to be parallel in the flip-non-flip plane. So far these tests have been performed only in the ρ-meson region where we know that possible non-flip terms are small at low $|t|$, but the errors are large[2].

In the region $t \approx t_{min}$, small non-flip terms are added according to the absorption model in order to obtain the t-dependence at threshold demanded by angular momentum conservation. With these assumptions, the phase angle between the m = 0 amplitude and the helicity-one unnatural exchange contribution can be determined from the data. This angle was found to be consistent with zero (phase coherence) at $|t| < 0.15$ GeV^2 by Estabrooks et al.[10] for the ρ-meson region and by Ochs[3] for ππ masses $600 < M_{\pi\pi} < 1900$ MeV.

With these two assumptions we parametrize in the t-channel the m = 0 amplitudes as in Ref. 3):

$$g_0^\ell = \frac{\sqrt{-t}}{M_\pi^2 - t} e^{b_0^\ell t} \cdot A_\ell(M_{\pi\pi}) ,$$

and the unnatural $|m| = 1$ amplitudes:

$$\frac{1}{\sqrt{2}} (g_1^\ell - g_{-1}^\ell) = g_-^\ell = \frac{-C_A^\ell(M_{\pi\pi})}{M_{\pi\pi}\sqrt{2}} e^{b_-^\ell t} \cdot \sqrt{\ell(\ell+1)} \cdot A_\ell(M_{\pi\pi}) ,$$

where g_m^ℓ, b_m^ℓ, C_A^ℓ, are the amplitudes, slopes, and absorption parameters for a particular spin ℓ and magnetic quantum number m. For the natural $|m| = 1$ amplitudes we assume $|g_+^\ell| = |g_-^\ell|$ *). A_ℓ describes the part of the amplitudes which depends only on ππ scattering and is expressed in terms of the T-matrix T_ℓ:

$$A_\ell(M_{\pi\pi}) = \frac{M_{\pi\pi}}{\sqrt{q}} \sqrt{2\ell+1} \cdot T_\ell$$

which, decomposed into isospin

$$T_\ell = \begin{cases} \frac{2}{3} T_\ell^0 + \frac{1}{3} T_\ell^2 & \ell \text{ even} \\ T_\ell^1 & \ell \text{ odd} , \end{cases}$$

can be expressed in phase shifts δ_ℓ^I and elasticities η_ℓ^I:

$$T_\ell^I = \frac{1}{2i} (\eta_\ell^I e^{2i\delta_\ell^I} - 1) .$$

---

*) Small (s-channel) non-flip terms can be introduced in order to obtain the t-dependence demanded by angular momentum conservation by writing (in the t-channel)

$$g_0^{NF} = g_0^\ell ; \quad g_0^{FL} = 0 ; \quad g_-^{NF} = \sqrt{\frac{t'}{t}} \cdot g_-^\ell ; \quad g_-^{FL} = \sqrt{\frac{t_{min}}{t}} \cdot g_-^\ell$$

$$g_+^{NF} = g_-^\ell ; \quad g_+^{FL} = 0 . \qquad (t' = t - t_{min})$$

Only $|g_+|$ enters in the calculation; its phase and flip-non-flip partition are set arbitrarily.

It is known experimentally[2,7,11] that C_A^ℓ decreases with $M_{\pi\pi}$. We introduce the ansatz

$$C_A^\ell(M_{\pi\pi}) = \bar{C}_A^\ell\{1 - \alpha\cdot(M_{\pi\pi} - \bar{M})\} ,$$

where we fit the same α for all spins ℓ, but independent values of $\bar{C}_A^\ell$ for different spins; $\bar{M}$ is the mean value of the $\pi\pi$ mass in the fitted mass region.

The phase shifts and elasticities were fitted in each $M_{\pi\pi}$ bin for the lower spins, while the higher waves (D-, F-waves for $M_{\pi\pi} < 1.6$ GeV, F-wave for $M_{\pi\pi} >$ > 1.6 GeV) were parametrized as Breit-Wigner functions. Partial waves with $\ell > 3$ were neglected, as suggested by the absence of higher moments in the data[2]. For spin 3 we write

$$T_3^1 = \frac{x_g M_g \Gamma}{M_g^2 - M_{\pi\pi}^2 - iM_g\Gamma} ,$$

$$\Gamma = \Gamma_g \left(\frac{q}{q_g}\right)^7 \frac{D_3(q_g R_g)}{D_3(qR_g)} ,$$

using the function

$$D_3(\xi) = 225 + 45\xi^2 + 6\xi^4 + \xi^6 .$$

M_g, Γ_g, x_g are the mass, width, and elasticity of the g meson. The subscript g refers to values at the g-meson mass.

For the f meson, background terms had to be introduced in the Breit-Wigner formula so as to be able to join smoothly to the value $\eta_2^0 \approx 0.8$ at 1.6 GeV, which was found from fitting the higher mass region 1.6-1.8 GeV using binned values for δ_2^0, η_2^0.

Identically to Ref. 3 we add constant background terms γ_{ij} with a K-matrix formalism, writing for $\pi\pi \to \pi\pi, K\bar{K}$

$$T_2^0 = \frac{K_{\pi\pi}q^5 - i(qk)^5(K_{\pi\pi}K_{KK} - K_{\pi K}^2)}{1 - (qk)^5(K_{\pi\pi}K_{KK} - K_{\pi K}^2) - i(q^5K_{\pi\pi} + k^5K_{KK})} ,$$

$$k = \sqrt{\frac{1}{4}M_{\pi\pi}^2 - M_K^2} ,$$

where M_K is the mass of the K meson. As pointed out in Ref. 3 the "KK channel" parametrizes in fact all inelastic channels:

$$K_{ij} = \frac{\gamma_i \gamma_j}{M_f^2 - M_{\pi\pi}^2} + \gamma_{ij}$$

$$\gamma_\pi^2 = \frac{M_f \Gamma_f}{q^5} x_f \frac{D_2(q_f R_f)}{D_2(q R_f)}$$

$$\gamma_K^2 = \frac{M_f \Gamma_f}{k_f^5} (1 - x_f) \frac{D_2(k_f R_f)}{D_2(k \cdot R_f)} .$$

The f- and g-meson effective radii are set to

$$R_f^2 = R_g^2 = 25.3 \text{ GeV}^{-2} ,$$ corresponding to an effective range of 1 fermi

$$D_2(\xi) = 9 + 3\xi^2 + \xi^4 ,$$

where M_f, Γ_f, x_f are the mass, width, and elasticity of the f-meson. For I = 2 S- and D-waves, we fit scattering length formulae to our experimental values[12]:

$$\delta_0^2 = -q/(1.1 + 0.88407q^2)$$

$$\delta_2^2 = -q^5 \Big/ \Big[(0.03351 + 0.236q^2)\cdot(1 + \frac{1}{3} r^2 q^2 + \frac{1}{9} r^4 q^4)\Big]$$

again with $r^2 = 25.3$ GeV^{-2}, δ_0^2, δ_2^2 in radian, all masses and momenta in GeV. The resulting curves are shown in Fig. 1, together with the results of some recent experiments[13].

Finally, using the above parametrizations, we can express the moments of the angular distribution $\langle Y_\ell^m \rangle$ as functions of $M_{\pi\pi}$ and t.

These calculated moments were fitted to the 13 measured moments $N\langle Y_\ell^m \rangle (\ell \leq 6, m \leq 1)$ determined in 40 MeV mass bins and 19 t-bins ($|t| < 0.16$ GeV^2).

For S- and P-waves (and D-waves with $M_{\pi\pi} > 1.6$ GeV) we fit independent δ_ℓ, η_ℓ in each mass bin. For all other parameters one value was fitted over each of four mass regions ($1 < M_{\pi\pi} < 1.16$; $1.16 < M_{\pi\pi} < 1.4$; $1.4 < M_{\pi\pi} < 1.6$; $1.6 < M_{\pi\pi} <$ < 1.8 GeV).

Therefore we have three different types of parameters:

a) b_0^ℓ, b_-^ℓ, $\bar{C}_A^\ell$ $(\ell = 0,3)$, α

describing the t-dependence of the process and allowing for a small change of the strength of absorption with $M_{\pi\pi}$;

b) M_g, Γ_g, x_g,

and for $M_{\pi\pi} < 1.6$ GeV: M_f, Γ_f, x_f, $\gamma_{\pi\pi}$, $\gamma_{\pi K}$, γ_{KK}

which fix the over-all phase by describing the leading resonances by Breit-Wigner formulae; and finally

c) δ_ℓ, η_ℓ $\quad \ell = 0,1 \quad M_{\pi\pi} < 1.6$ GeV
$\ell = 0,1,2 \quad M_{\pi\pi} > 1.6$ GeV ,

giving an energy independent description of the lower-lying partial waves.

No attempt was made to impose smooth transitions between different mass regions.

3. DISCUSSION OF THE AMBIGUITIES

In the absence of total $\pi\pi$ cross-section measurements the over-all phase of the amplitudes cannot be determined. The only simple possibility is to assume a Breit-Wigner behaviour of the leading resonances (f,g) in the mass regions where they dominate, and interpolate smoothly in between.

We want to stress that our solutions for the phase shifts depend strongly on this assumption; deviations from the Breit-Wigner shape, in particular an over-all phase depending on the $\pi\pi$ scattering angle θ, might lead to quite different results[14].

If we then limit the discussion to a finite number of waves (we assume spin $\ell \leq 3$ for $M_{\pi\pi} < 1.8$ GeV) we encounter only a finite number of discrete ambiguities which can be formulated with the help of Barrelet zeros[15]. For maximal spin $L_{max} = 3$ we can write the $\pi\pi$ cross-section (θ is the scattering angle):

$$\sigma_{\pi\pi} \propto (\cos\theta - z_1)(\cos\theta - z_2)(\cos\theta - z_3) \times$$
$$\times (\cos\theta - z_1^*)(\cos\theta - z_2^*)(\cos\theta - z_3^*) \ .$$

The experiment measures the cross-section, and if we want to determine the amplitudes, we can take z_ℓ or z_ℓ^* ($\ell = 1, \ell_{max}$); therefore we have $2^{\ell_{max}} = 8$ ambiguities for $\ell_{max} = 3$.

One half of these ambiguities can be eliminated, if the higher phase shift (δ_D or δ_F) is small and assumed to be positive (as expected for a Breit-Wigner behaviour) in a region where some of the lower phase shifts are large[4,16].

We expect therefore two solutions in the mass region of the f meson and four solutions in the g-meson region.

In principle, the $m \geq 1$ moments do not have these ambiguities; in practice, however, they change z_ℓ slightly, but do not help to resolve the ambiguities.

4. RESULTS OF THE FIT

From the phase shifts obtained in the fit, one can calculate the zeros z_ℓ. The imaginary parts Im z_ℓ are shown in Fig. 2. The error bars give the range of values found for different fits. Once we have found one solution, we can calculate the zero positions, take the other signs of the imaginary parts, and calculate δ, η of the other solutions.

These values have to be used as starting points of new fits, since the m = 0 moments break the symmetry. This fact explains why the different solutions do not give exact mirror images of the imaginary parts.

We classify the different solutions according to the sign of Im z_ℓ in the region $M_{\pi\pi} \sim 1.5$ GeV, assuming that Im z_1 changes sign around $M_{\pi\pi} = 1.22$ GeV. Solutions where Im z_1 does not change sign at this mass cannot be ruled out, and can be obtained by connecting solutions with different Im z_1 and equal Im z_2, Im z_3 at $M_{\pi\pi} = 1.22$ GeV.

Below $M_{\pi\pi} = 1.4$ GeV two solutions are possible; at 1.4 GeV, Im z_2 goes close to zero, stays negative, or crosses over introducing a further ambiguity which then leads to four solutions. At $M_{\pi\pi} \approx 1.78$ GeV new ambiguities arise which cannot be studied with our data.

We show the various solutions in the following figures. The solution (---) [i.e. all Im z_ℓ (1.5) negative] (Fig. 3) shows apart from the f and g mesons, a slowly rising S-wave going through 90° under the f meson, and a rapid drop of the elasticity under the g meson which could not be described with a simple resonance form. The P-wave looks like the tail of the ρ meson.

The next solution (-+-) (Fig. 4) corresponds to Im z_2 starting negative and crossing zero at $M_{\pi\pi} = 1.4$ GeV. This solution shows an inelastic S-wave resonance under the g meson and a rise of the D-wave in the same region.

Solution (+--) (Fig. 5) has an Im z_1 starting negative at $M_{\pi\pi} = 1$ GeV and crossing zero at 1.22 GeV. In the region $M_{\pi\pi} \approx 1.1$ GeV it is identical to the solution found by Protopopescu et al.[17].

Around 1.4 GeV the S-wave becomes unphysical; therefore we think we can rule out this solution, which shows an inelastic P-wave resonance. We want to point out that if we introduce inelastic isospin-2 waves, the I = 0 S-wave will become even more unphysical. However, it is probably possible to deform the Breit-Wigner shape of the f meson far enough to make this solution physical. We can, of course, take this solution below 1.22 GeV and connect it with solution (---) above this ππ mass*).

At 1.4 GeV, Im z_2 can also cross zero, which leads to solution ++- (Fig. 6). The S-wave elasticity is still larger than one at three points below 1.4 GeV; however, in the fit it was possible to constrain the elasticity to values smaller than one, leading to worse but not unacceptable values of χ^2. We therefore feel that this solution is somewhat less probable than the two other possibilities, but it cannot be ruled out at present. This solution has a very rapidly rising S-wave going through 90° and an inelastic, broad P-wave resonance under the g meson.

---

*) We have seen preliminary data of the reaction $\pi^- p \to \pi^0\pi^0 n$ from the Karlsruhe-Pisa group[18] which probably will be able to resolve the ambiguity around 1.1 GeV.

Values of the resonance parameters and the absorption constants $\bar{C}_A^{\ell}$ are given in Tables 1 and 2.

Since the S-wave is different for these ambiguous solutions, they can, in principle, be resolved by studying the reaction $\pi^- p \to \pi^0\pi^0 n$. Unfortunately the available data are not sufficient.

If we compare our present solutions with the phase shifts published one year ago[3], we see that these correspond almost exactly to our new solution (---) below 1.4 GeV, but switch to our new solution (+--) at $\sim$ 1.5 GeV, which then leads to P-wave structure.

In Figs. 7, 8, and 9 we show projections of the fit of solutions (---) with the measured moments in the interval $0.01 < |t| < 0.16$ GeV^2. We note the considerable improvement of the new fits compared to the old energy-dependent fits shown in Fig. 10, particularly for $N\langle Y_4^0\rangle$.

We attempted to get a measure for the probability that Im z_1 crosses zero at 1.5 GeV by fixing the S- and P-wave phase shifts and elasticity at the two lower points at 1.42 and 1.46 GeV to our solution (---), and at the two highest points at 1.54 and 1.58 to our (+--).

The S- and P-waves at 1.5 GeV were varied together with the f- and g-meson Breit-Wigner parameters, constraining the solution to a fixed value of Im z_1.

In Fig. 11 we show the χ^2 profile as a function of Im z_1 (1.5 GeV). We see two distinct minima at ±0.12, but no intermediate minimum around zero. We therefore conclude from our new fits that Im z_1 does not cross zero at 1.5 GeV, and thus the solution of Ref. 3 is ruled out in this mass region. This improved discrimination was achieved by using both more stringent constraints on fits in larger mass bins and the complete error matrix.

Looking at all solutions, we see that Im z_2 (1.5) < 0 has no S-wave resonance under the g meson, Im z_2 (1.5) > 0 has one. Similarly Im z_1 (1.5) < 0 has no P-wave resonance under the g meson, whereas Im z_1 (1.5) > 0 has one (but with bad χ^2).

Estabrooks and Martin[4] have so far published two solutions found in their analysis of the same data. There is qualitative agreement of their solution A with our (---) and, above 1.22 GeV, of their solution B with our (+--). They exclude our (+--) below 1.22 GeV using data from $\pi^- p \to K^+K^- n$. We believe that so far no unambiguous decision can be taken, but we expect that already existing $\pi^0\pi^0$ data will be able to distinguish between these ambiguities.

An interesting method for resolving the ambiguities has been presented by Shimada[16]. He shows that only solution (---) does not induce anomalous behaviour of the amplitude zeros in other charge configurations.

5. CONCLUSION

With our present data we were able to limit $\pi\pi$ scattering below 1.8 GeV to four more or less favourable solutions. Nevertheless the question of the existence of daughter trajectories can only be settled after an unambiguous set of phase shifts is found. This determination will have to wait for further experimental data, particularly in the reactions

$$\begin{aligned} \pi^- p &\to \pi^0 \pi^0 n \\ &\to \pi^- \pi^0 p \ . \end{aligned}$$

REFERENCES

1) J.T. Caroll, R.N. Diamond, M.W. Firebaugh, W.D. Walker, J.A.J. Mathews, J.D. Prentice and T.S. Yoon, Phys. Rev. Letters 25, 318 (1972).
G. Grayer, B. Hyams, C. Jones, P. Schlein, W. Blum, H. Dietl, W. Koch, E. Lorenz, G. Lütjens, W. Männer, J. Meissburger, W. Ochs, U. Stierlin and P. Weilhammer, Proc. 3rd Internat. Conf. on Experimental Meson Spectroscopy, Philadelphia, 1972 (AIP Conf. Proc. No. 8, Particles and Fields Subseries No. 3), p. 5.

2) G. Grayer, B. Hyams, C. Jones, P. Schlein, P. Weilhammer, W. Blum, H. Dietl, W. Koch, E. Lorenz, G. Lütjens, W. Männer, J. Meissburger, W. Ochs and U. Stierlin, Nuclear Phys. B75, 189 (1974).

3) W. Ochs, Thesis, Ludwig-Maximilians-Universität, Munich (1973).
B. Hyams, C. Jones, P. Weilhammer, W. Blum, H. Dietl, G. Grayer, W. Koch, E. Lorenz, G. Lütjens, J. Meissburger, W. Ochs, U. Stierlin and F. Wagner, Proc. Internat. Conf. on ππ Scattering and Associated Topics, Florida State Univ., Tallahassee, 1973 (AIP Conf. Proc. No. 13, Particles and Fields Subseries No. 5), p. 206; and Nuclear Phys. B64, 134 (1973).

4) W. Männer, New results in ππ scattering, 4th Internat. Conf. on Experimental Meson Spectroscopy, Boston, 1974 (AIP Conf. Proc. No. 21, Particles and Fields Subseries No. 8), p. 22.

5) P. Estabrooks and A.D. Martin, Phys. Letters 53B, 253 (1974).

6) G.F. Chew and F.E. Low, Phys. Rev. 113, 1640 (1959).

7) B. Hyams, C. Jones, P. Weilhammer, W. Blum, H. Dietl, G. Grayer, E. Lorenz, G. Lütjens, W. Männer, J. Meissburger, W. Ochs and U. Stierlin, Phys. Letters 51B, 272 (1974).

8) G.L. Kane and M. Ross, Phys. Rev. 177, 2353 (1969).
P.K. Williams, Phys. Rev. D1, 1313 (1970).
G.C. Fox, *in* Proc. Conf. on Phenomenology in Particle Physics, Calif. Inst. Tech., Pasadena, 1971 (Calif. Inst. Tech., Pasadena, 1971), p. 703.

9) G. Grayer, B. Hyams, C. Jones, P. Weilhammer, W. Blum, H. Dietl, W. Koch, E. Lorenz, G. Lütjens, W. Männer, J. Meissburger, W. Ochs and U. Stierlin, Nuclear Phys. B50, 29 (1972).

10) P. Estabrooks, A.D. Martin, G. Grayer, B. Hyams, C. Jones, P. Weilhammer, W. Blum, H. Dietl, W. Koch, E. Lorenz, G. Lütjens, W. Männer, J. Meissburger and U. Stierlin, Proc. Internat. Conf. on ππ Scattering and Associated Topics, Florida State Univ., Tallahassee, 1973 (AIP Conf. Proc. No. 13, Particles and Fields Subseries No. 5), p. 37.

11) W. Ochs and F. Wagner, Phys. Letters 44B, 271 (1973).

12) W. Hoogland, G. Grayer, B. Hyams, C. Jones, P. Weilhammer, W. Blum, H. Dietl, W. Koch, E. Lorenz, G. Lütjens, W. Männer, J. Meissburger and U. Stierlin, Nuclear Phys. B69, 266 (1974).

13) F. Wagner, Meson Spectroscopy, Rapporteur's talk at the 17th Internat. Conf. on High-Energy Physics, London, 1974 (Rutherford Lab., Chilton, Didcot, England, 1974), p. II-27.

14) For the use of fixed-t-dispersion relations in this context see:
C.D. Froggatt and J.L. Petersen, Phase-shift analysis of $\pi^+\pi^-$ scattering between 1.1 and 1.8 GeV based on fixed momentum transfer analyticity, NORDITA-75/2 (1975).

15) E. Barrelet, Nuovo Cimento 8A, 331 (1972).

16) T. Shimada, Univ. of Tokyo, preprint UT-245, Dec. 1974.

17) S.D. Protopopescu, M. Alston-Garnjost, A. Barbaro-Galtieri, S.M. Flatté, J.H. Friedman, T.A. Lasinski, G.R. Lynch, M.S. Rabin and F.T. Solmitz, Proc. 3rd Internat. Conf. on Experimental Meson Spectroscopy, Pennsylvania, Philadelphia, 1972 (AIP Conf. Proc. No. 8, Particles and Fields Subseries No. 3), p. 17.

18) H. Müller, private communication.

Table 1

f- and g-meson resonance parameters for the different solutions

Solution	M_f	Γ_f	x_f	M_g	Γ_g	x_g
−−−	1.279 ± 0.001	0.192 ± 0.001	0.806 ± 0.002	1.725 ± 0.003	0.296 ± 0.01	0.251 ± 0.003
−+−	1.279 ± 0.001	0.192 ± 0.001	0.806 ± 0.002	1.719 ± 0.001	0.253 ± 0.006	0.228 ± 0.004
+−−	1.271 ± 0.001	0.181 ± 0.002	0.810 ± 0.002	1.721 ± 0.002	0.240 ± 0.008	0.228 ± 0.002
++−	1.272 ± 0.001	0.184 ± 0.003	0.801 ± 0.005	1.720 ± 0.001	0.239 ± 0.006	0.235 ± 0.002

Table 2

Absorption parameters C_A of P-, D-, and F-waves for the different solutions

Mean $M_{\pi\pi}$	Solution	$C_A(P)$	$C_A(D)$	$C_A(F)$
1.08	−±−	0.81 ± 0.05	0.92 ± 0.03	1.8 ± 0.3
	+±−	0.87 ± 0.02	0.88 ± 0.02	0.86 ± 0.05
1.28	−±−	0.62 ± 0.02	0.69 ± 0.02	1.04 ± 0.01
	+−−	0.65 ± 0.04	0.68 ± 0.01	1.08 ± 0.10
	++−	0.64 ± 0.05	0.70 ± 0.01	1.15 ± 0.10
1.50	−−−	0.38 ± 0.08	0.55 ± 0.03	1.03 ± 0.06
	−+−	0.49 ± 0.08	0.54 ± 0.02	0.91 ± 0.05
	+−−	0.37 ± 0.03	0.53 ± 0.02	1.35 ± 0.05
	++−	0.48 ± 0.03	0.54 ± 0.03	0.97 ± 0.05
1.70	−−−	0.29 ± 0.05	0.35 ± 0.03	0.56 ± 0.03
	−+−	0.59 ± 0.32	0.65 ± 0.07	0.53 ± 0.02
	+−−	0.54 ± 0.05	0.20 ± 0.04	0.61 ± 0.02
	++−	0.47 ± 0.10	0.57 ± 0.13	0.54 ± 0.02

Figure captions

Fig. 1 : I = 2 S- and D-wave phase shifts from Ref. 13. The curves are obtained with the parametrization used in our fits.

Fig. 2 : Imaginary parts of Barrelet zeros as obtained from the fits. Error bars indicate the range of values for different solutions.

Fig. 3 : Solution (---).

Fig. 4 : Solution (-+-).

Fig. 5 : Solution (+--).

Fig. 6 : Solution (++-).

Fig. 7 : Mass spectrum and unnormalized moments $N\langle Y_1^0\rangle$, $N\langle Y_1^1\rangle$, $N\langle Y_2^0\rangle$, $N\langle Y_2^1\rangle$ in $0.01 < |t| < 0.16$ GeV^2 for solution (---). The hand-drawn curves connect the results of the different mass bins summed over t.

Fig. 8 : Unnormalized moments $N\langle Y_3^0\rangle$, $N\langle Y_3^1\rangle$, $N\langle Y_4^0\rangle$, $N\langle Y_4^1\rangle$ in $0.01 < |t| < 0.16$ with projection of fit for solution (---).

Fig. 9 : Unnormalized moments $N\langle Y_5^0\rangle$, $N\langle Y_5^1\rangle$, $N\langle Y_6^0\rangle$, $N\langle Y_6^1\rangle$ GeV^2 in $0.01 < |t| <$ < 0.16 with projection of fit for solution (---).

Fig. 10 : Unnormalized moments with fitted curve from Ref. 3.

Fig. 11 : χ^2 profile for 1198 degrees of freedom as a function of Im z_1 (1.5 GeV) for a solution changing from --- to +-- at 1.5 GeV.

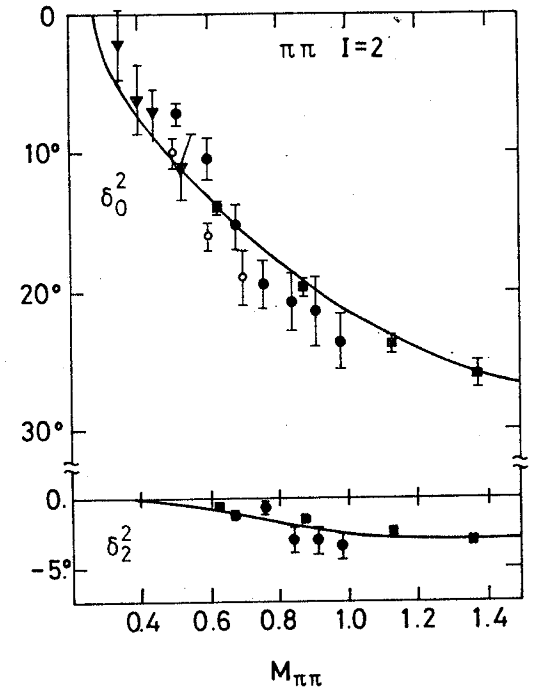
ππ I=2
δ_0^2
δ_2^2
0
10°
20°
30°
0.
-5°
0.4
0.6
0.8
1.0
1.2
1.4
$M_{\pi\pi}$

Fig. 1

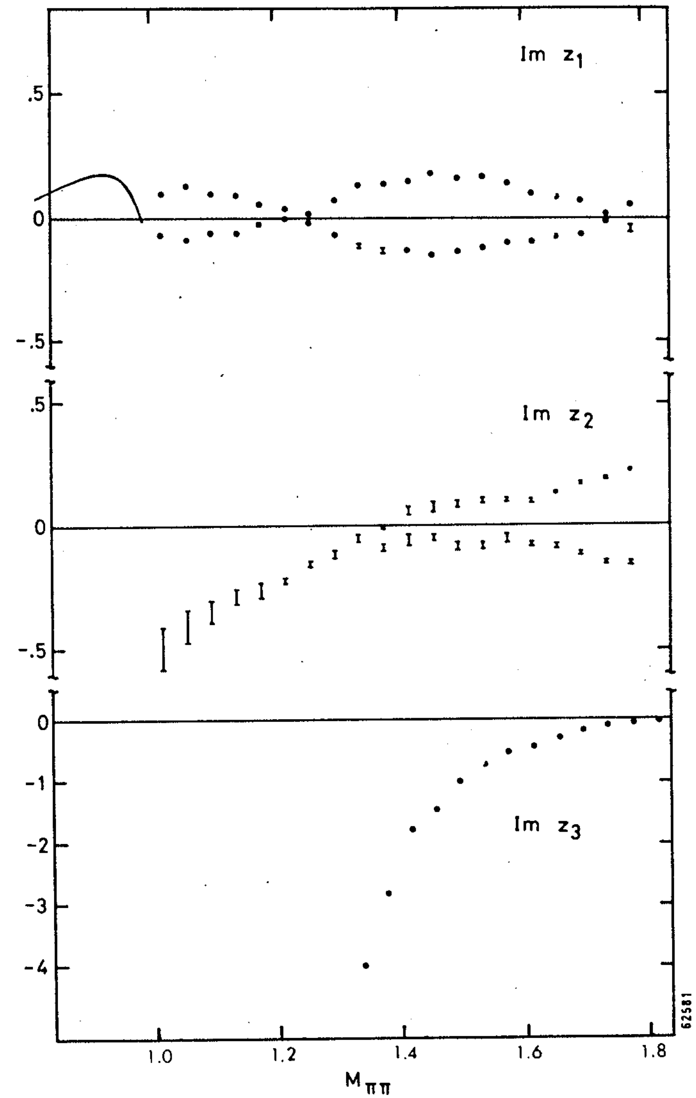
Im z_1
Im z_2
Im z_3
.5
0
-.5
-1
-2
-3
-4
1.0
1.2
1.4
1.6
1.8
$M_{\pi\pi}$
62581

Fig. 2

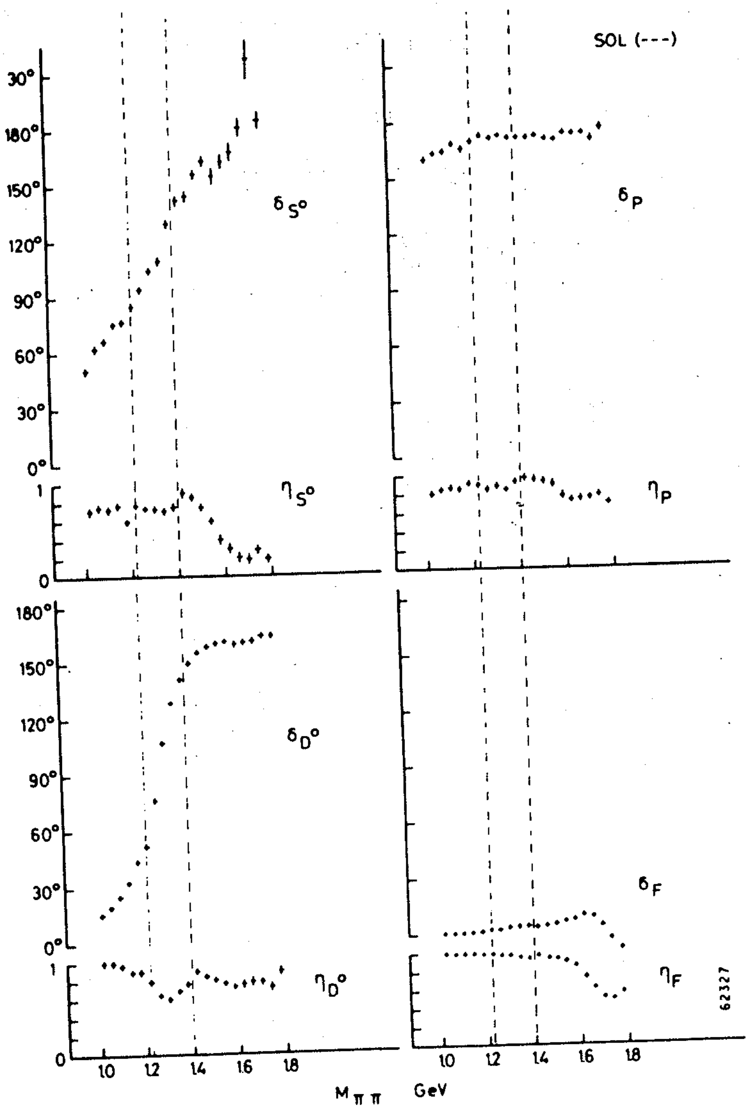

SOL (---)
30°
180°
150°
120°
90°
60°
30°
0°
δ_S°
δ_P
η_S°
η_P
δ_D°
δ_F
η_D°
η_F
1
0
1.0 1.2 1.4 1.6 1.8
$M_{\pi\pi}$ GeV
62327

Fig. 3

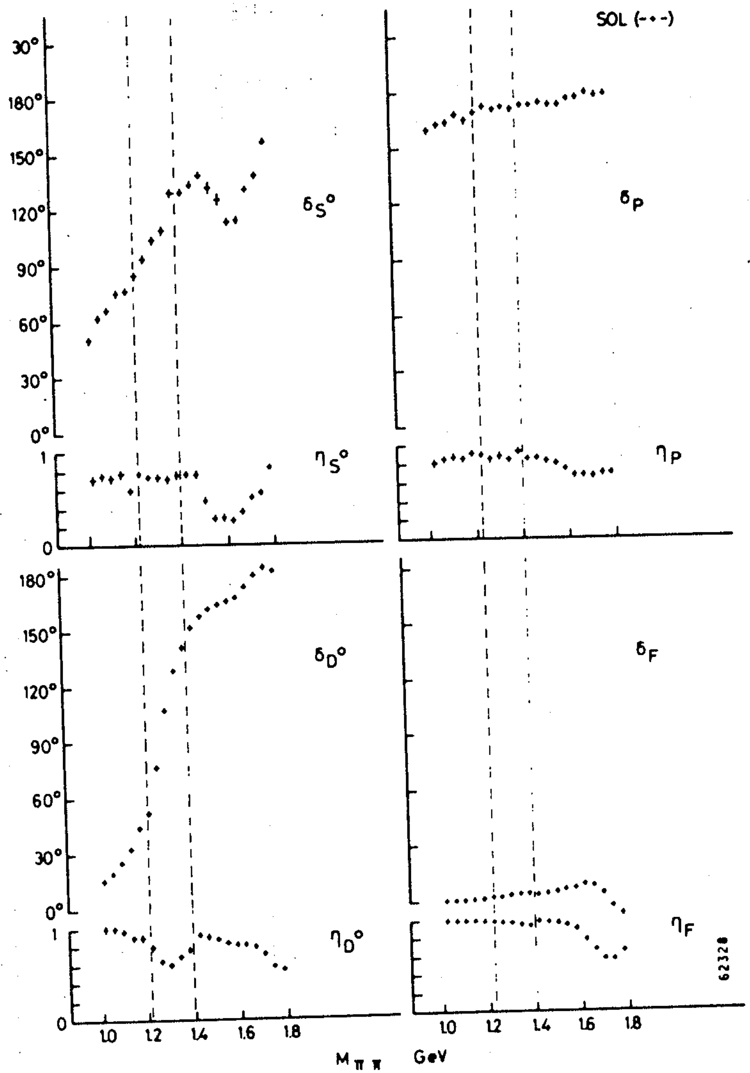

SOL (-·-)
30°
180°
150°
120°
90°
60°
30°
0°
δ_S°
δ_P
η_S°
η_P
δ_D°
δ_F
η_D°
η_F
1
0
1.0 1.2 1.4 1.6 1.8
$M_{\pi\pi}$ GeV
62328

Fig. 4

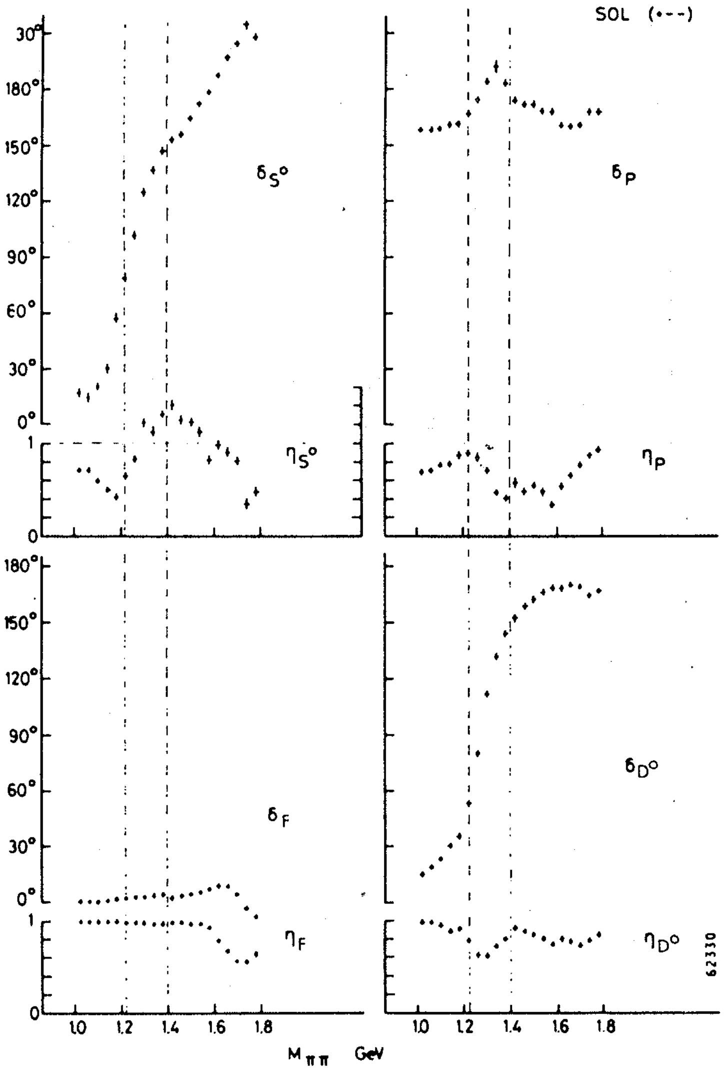

SOL (---)
δ_S°
η_S°
δ_P
η_P
δ_F
η_F
δ_D°
η_D°
$M_{\pi\pi}$ GeV
62330

Fig. 5

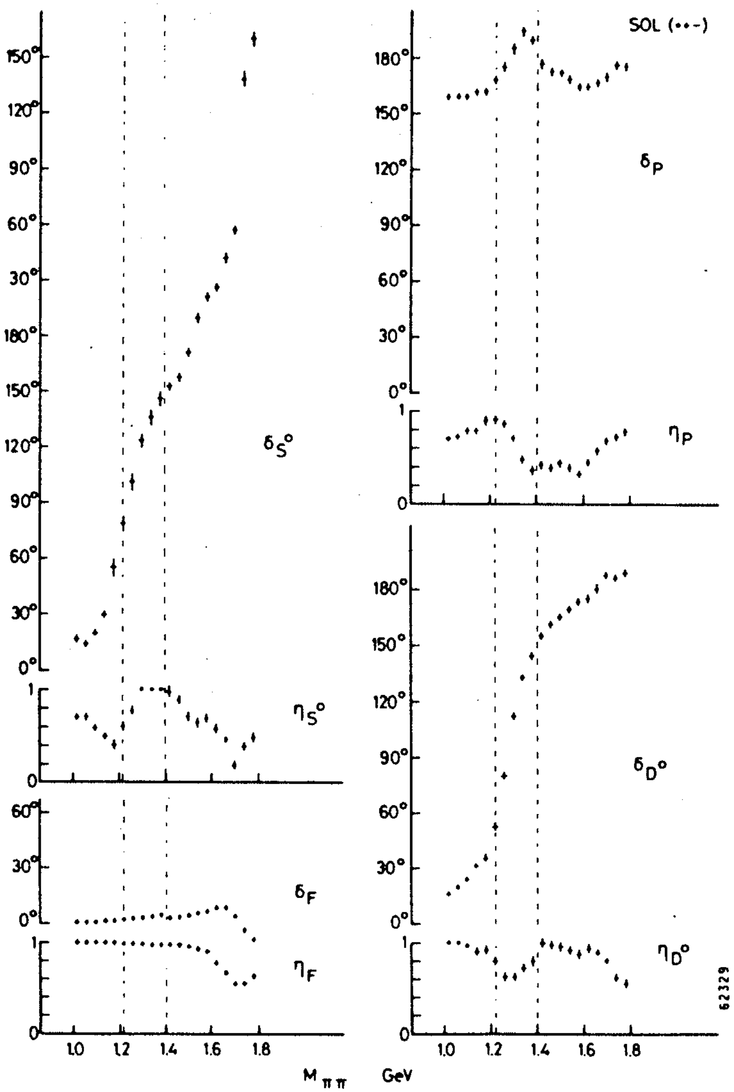

SOL (•••-)
δ_S°
η_S°
δ_P
η_P
δ_F
η_F
δ_D°
η_D°
$M_{\pi\pi}$ GeV
62329

Fig. 6

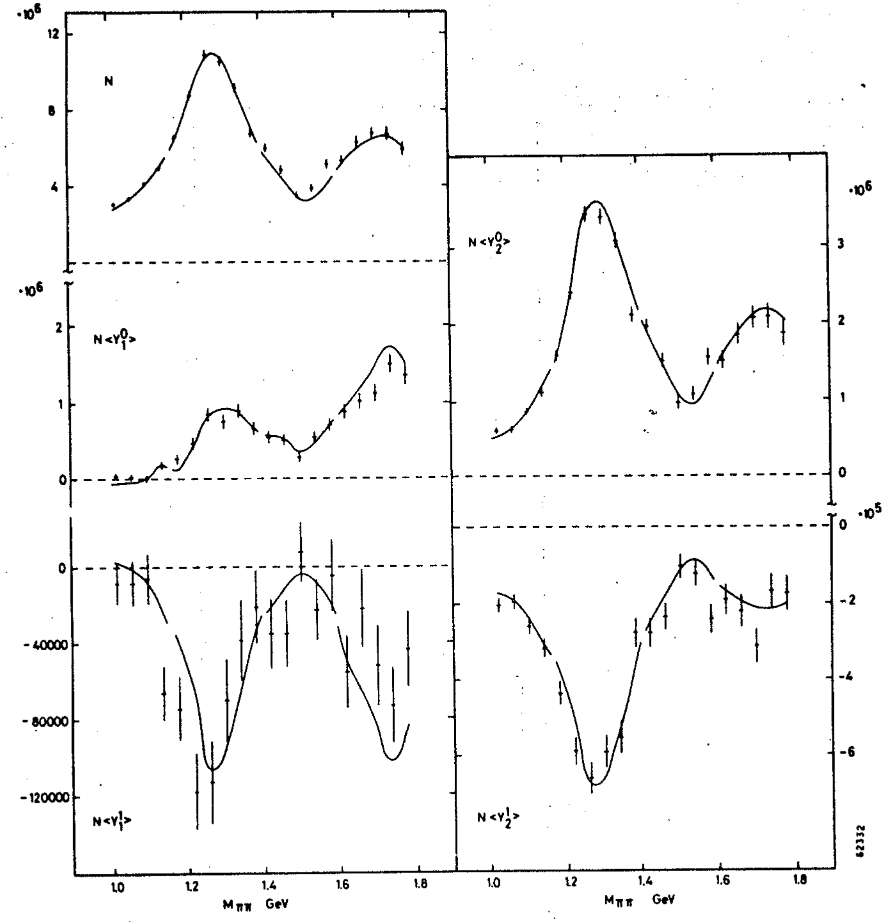

Fig. 7

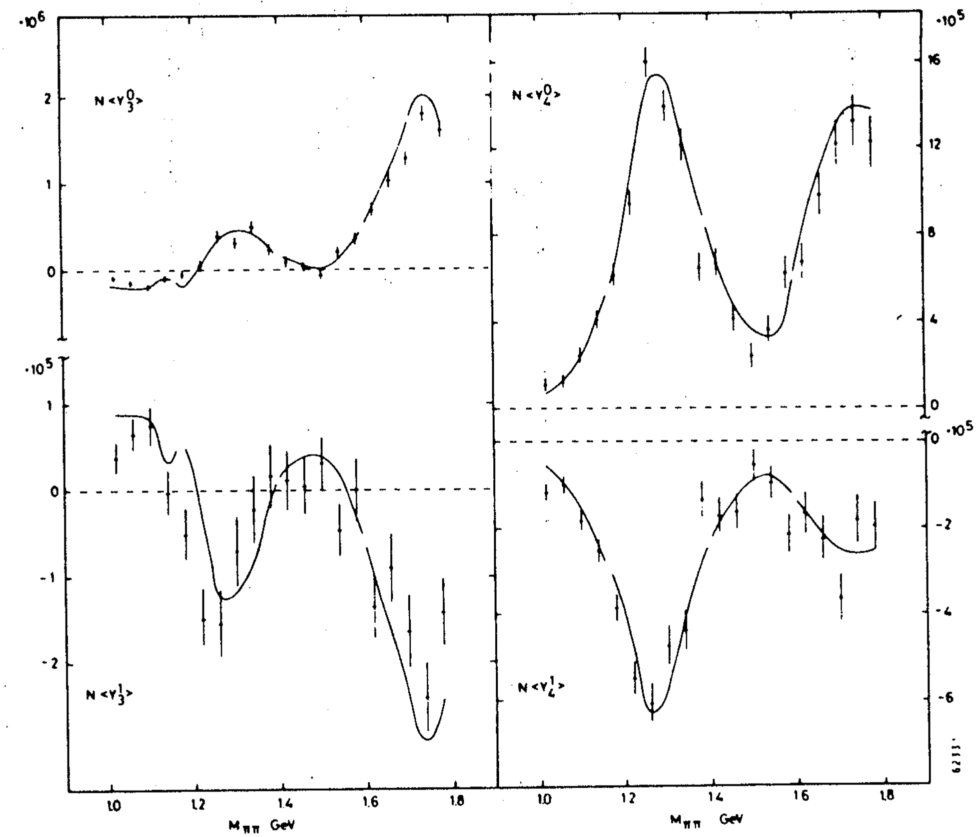

Fig. 8

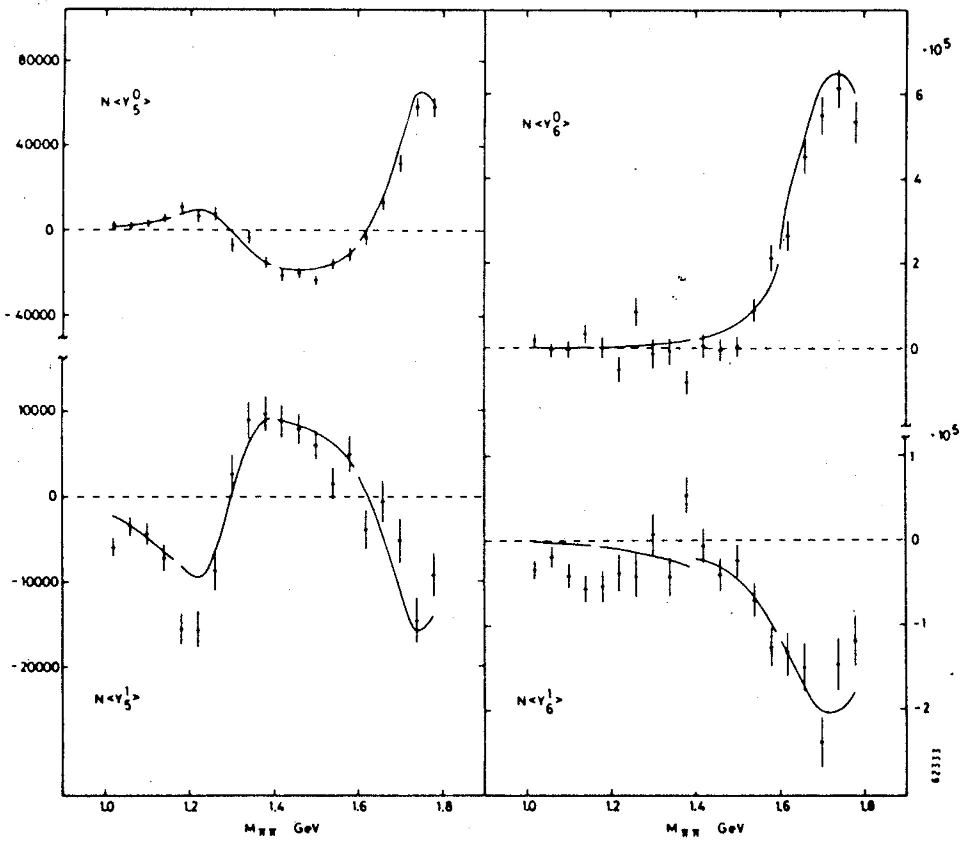

80000
40000
0
-40000
10000
0
-10000
-20000
$N\langle Y_5^0\rangle$
$N\langle Y_5^1\rangle$
$N\langle Y_6^0\rangle$
$N\langle Y_6^1\rangle$
$\cdot 10^5$
6
4
2
0
$\cdot 10^5$
1
0
-1
-2
1.0
1.2
1.4
1.6
1.8
$M_{\pi\pi}$ GeV
62333

Fig. 9

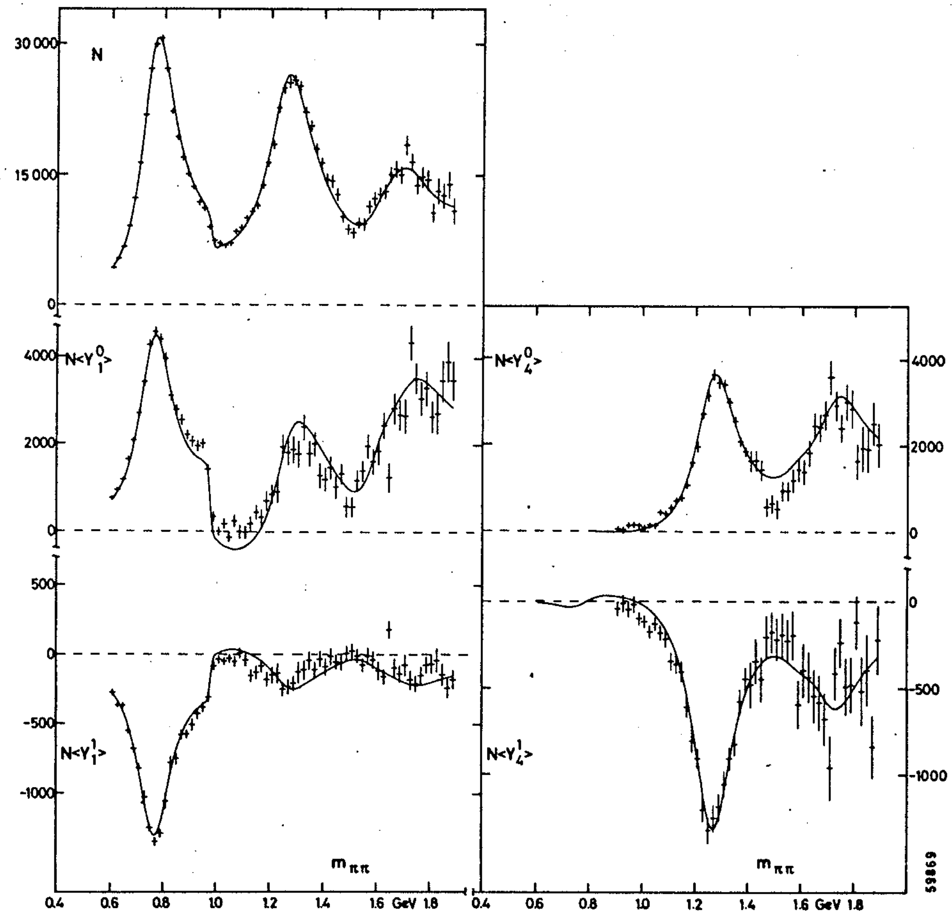

N
30 000
15 000
0
$N\langle Y_1^0\rangle$
4000
2000
0
500
0
-500
-1000
$N\langle Y_1^1\rangle$
$N\langle Y_4^0\rangle$
$N\langle Y_4^1\rangle$
$m_{\pi\pi}$
0.4
0.6
0.8
1.0
1.2
1.4
1.6 GeV
1.8
59869

Fig. 10

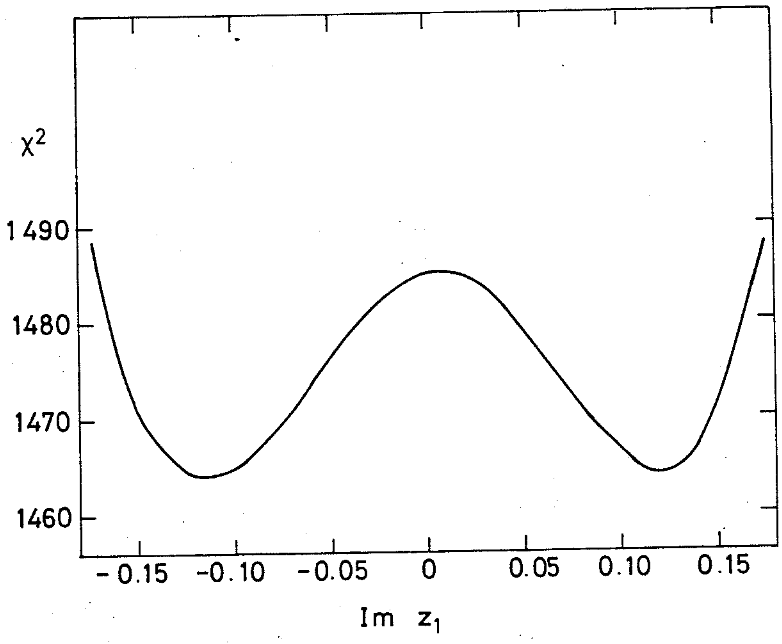

Fig. 11